Identification of Thomas Peaks in Coupled-Channel Calculations for Charge Transfer

Nobuyuki Toshima
Institute of Applied Physics, University of Tsukuba, Tsukuba, Ibaraki 305, Japan

Jörg Eichler[a]
Bereich Schwerionenphysik, Hahn-Meitner-Institut Berlin, D-1000 Berlin 39, Germany
(Received 30 August 1990)

It is demonstrated that the nonperturbative coupled-channel method can be efficiently extended to very-high-lying continuum states by using a sufficiently large basis set of Gaussian-type orbitals. In applying the method to the Thomas mechanism in $H^+ + H$ collisions at 5 MeV, we identify two distinct and interfering reaction paths, one via the target and one via the projectile continuum. We get remarkable agreement with experimental data.

PACS numbers: 34.70.+e

In 1927 Thomas[1] proposed a classical double-scattering mechanism for electron transfer at asymptotically high projectile velocities v. In the first step, the initially bound electron is scattered off the projectile by 60° thereby acquiring a speed equal to the projectile velocity. In the second step, the electron is elastically rescattered off the target nucleus by again 60°, so that it travels along with the projectile. Thirty-five years ago, Drisko[2] established the connection of this process with a quantum-mechanical description in a second-Born approximation. Since that time, the process has been reconsidered[3] in various degrees of approximations[4-8] and, even before it has been identified experimentally,[9,10] has played an eminent role in assessing the validity of capture theories. All theoretical treatments so far have remained within the framework of second-order perturbation theory except for recent classical-trajectory Monte Carlo calculations[11] in which the classical equations of motion for the three-body system are solved rigorously. In the present Letter we present the first *nonperturbative* quantum-mechanical calculations of the Thomas mechanism. While all previous theories usually assume a reaction path via the free-electron continuum we show that there are two equally important and interfering reaction paths, one via the target and one via the projectile Coulomb continuum.

Quite generally, there have been two lines of approach to charge transfer in energetic collisions. One is the perturbative approach which has the advantage that the particle continuum can be incorporated in a reasonable way but has the drawback that little is known about the convergence of a perturbation expansion. The other approach is the coupled-channel method[12] which treats the interactions to infinite order but does not easily allow one to incorporate continuum effects and thus fails to predict capture cross sections at high energies. In the current paper, we demonstrate how the coupled-channel method can be efficiently handled so that it is suitable for incorporating high-lying continuum states and hence constitutes a universally applicable nonperturbative method for treating energetic ion-atom collisions.

In the past, the coupled-channel method has usually been regarded as adequate for atomic collisions in the low- and intermediate-energy range[12] but untractable in the high-energy range, that is, when the projectile velocity considerably exceeds the orbital velocity of the active electron. The reason for this limitation can be understood from the fact that with increasing projectile velocity the interaction matrix elements assume an increasingly oscillatory behavior (caused by the translation factor[13]) which renders their numerical evaluation difficult if not impossible. This problem is avoided by using Gaussian-type orbitals (GTO) which allow for an analytical evaluation both of the single-center and the two-center matrix elements. For a long time, Gaussian basis expansions have been successfully used in quantum chemistry.[14] For atomic collisions,[15] the extension to traveling orbitals entails the continuation to complex variables. Formulas for the matrix elements have been given by Errea, Mendez, and Riera,[16] but only one recent application[17] is known to us, in which the interest is mainly focused on two-electron effects, namely, in $He^{++} + He$ and $He^+ + He^+$ collisions for energies up to 100 keV/u. Correspondingly, the number of GTO per electron had to be kept rather small.

In our case we consider charge transfer for $H^+ + H$ collisions at 5 MeV. Adopting the impact-parameter picture with a classical rectilinear trajectory for the projectile motion, we confine ourselves to s states which contain the highest momentum components and should be dominant at such a high collision energy. We use a basis set of eighty GTO, forty at the target and forty at the projectile, with a modified geometrical progression for the exponential coefficients α_i in the Gaussian dependence $\exp(-\alpha_i r^2)$. The modification is chosen in such a way that it increases the number of states with a *long* range $\bar{r} = 1/\alpha_i^{1/2}$. For typical calculations, the range parameter varies between $\bar{r} = 0.005$ and 20 a.u. By di-

agonalizing the single-center Hamiltonian we obtain the three lowest hydrogenic energy eigenvalues to a precision of better than 10^{-8} and the $4s$ state still with an accuracy of 10^{-5}. In most calculations we only keep the four lowest bound states $1s$, $2s$, $3s$, and $4s$ and in addition 21 continuum states reaching up to an energy of about 250 a.u., thus discarding unimportant states at still higher energies. As will become clear in Fig. 2, it is convenient to choose the starting point of the sequence of coefficients α_i so that after diagonalization, one of the discrete positive-energy eigenvalues coincides with the matching energy $E_m = \frac{1}{2} m_e v^2 = 100$ a.u. corresponding to a free electron traveling with the same speed as the 5-MeV proton. After having determined the forty GTO and the 25 eigenstates to be included, the overlap and the one- and two-center potential matrix elements at a given time during the collision can be calculated as finite sums over analytical expressions. These calculations are performed explicitly at 300 time steps for $t \geq 0$. By symmetry and interpolation, all additional values needed can also be obtained. The coupled equations then are solved with the initial condition that the electron initially occupies the $1s$ target state. At each step, the accuracy and convergence of the calculations are carefully checked.

In the Thomas mechanism as usually represented by

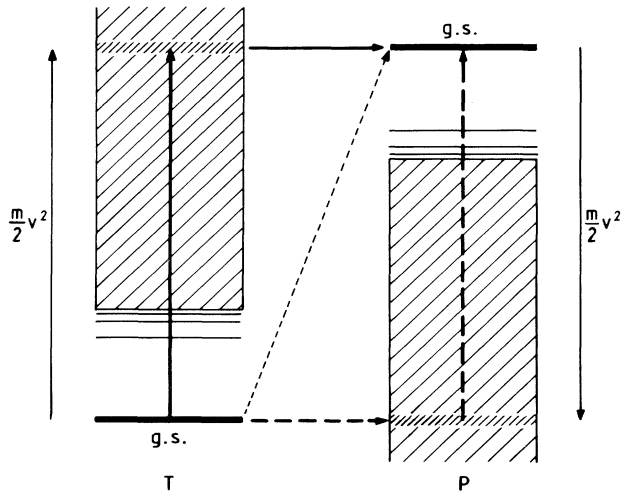

FIG. 1. Schematic diagram for the two-path Thomas mechanism. The energy spectra for the target (T) and the projectile (P) are plotted in such a way that they indicate the direction of the relevant momenta in the electronic Coulomb continuum. The solid arrows show a reaction path in which the target is first excited into a continuum state with a large momentum in the *forward* direction (with respect to the projectile motion) and with subsequent transfer into the projectile. The dashed arrows show the second path, in which transfer occurs into a projectile continuum state with a large momentum in the *backward* direction and subsequent deexcitation into the ground state (g.s.). The short-dashed line shows the nonresonant direct capture.

second-order perturbation theory,[2,4] the electron in the intermediate state propagates freely. In contrast, for a two-center Coulomb continuum it is possible to distinguish portions of the continuum centered around the target or centered around the projectile. Therefore, in Fig. 1 we present a schematic diagram for the charge-transfer reaction drawn to exhibit the symmetry between target and projectile. The $1s$ ground states of the collision partners are displaced by the energy $E_m = \frac{1}{2} m_e v^2$. Direct transitions (short-dashed arrow) are possible but are suppressed by the lack of appreciable overlap of the electronic momentum wave functions. For two-step processes, we may identify two reaction sequences. The solid arrows show the sequence where the target electron is excited into a high-lying continuum state with energy E_m and a longitudinal momentum along the direction of the projectile velocity. From there, the electron is resonantly (i.e., with momentum matching) transferred into the projectile ground state. The dashed arrows show the sequence where the electron is first transferred resonantly into a portion of the continuum centered around the projectile. In this case, the longitudinal momentum of the electron points *opposite* to the projectile velocity as seen from the projectile frame. In order to exhibit this feature it is suggestive to plot the energy diagram of the projectile upside down as has been done on the right-hand side of Fig. 1. The figure illustrates the two equivalent paths contributing to the Thomas mechanism with Coulomb intermediate states: The first path proceeds via the target continuum, while the second proceeds via the projectile continuum. Both paths will necessarily interfere.

In order to establish our new picture of a two-path mechanism we have performed a number of auxiliary calculations. In Fig. 2 we have plotted the probability

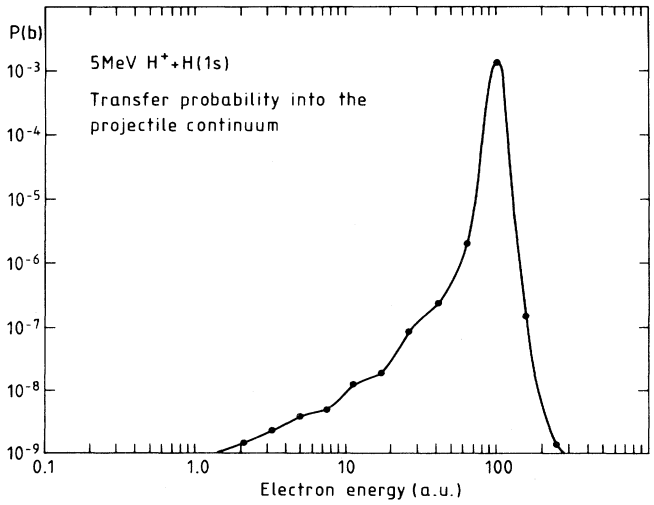

FIG. 2. Calculated transfer probability into the projectile continuum in a 5-MeV $H^+ + H$ collision at an impact parameter of $b = 0.36$ a.u.

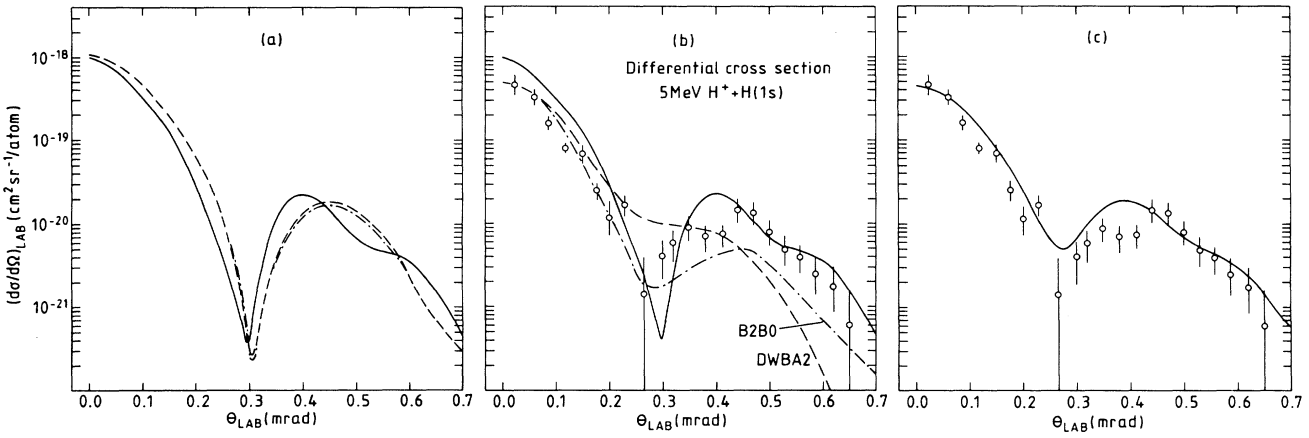

FIG. 3. Differential cross sections for charge transfer in 5-MeV $H^+ + H$ collisions. (a) Coupled-channel calculations: For the dashed curve the target continuum is omitted, for the dash-dotted curve the projectile continuum is omitted, and for the solid curve both Coulomb continua are included. (b) The solid curve represents the result of our coupled-channel calculations for capture into $1s$, $2s$, $3s$, and $4s$ states, the dash-dotted and the dashed curves give results of B2B0 and DWBA2 calculations, respectively, both satisfying Coulomb boundary conditions; see Refs. 7 and 8. In the latter cases, the $1s$-$1s$ cross sections have been multiplied with a factor of 1.202 to account for higher final states. The experimental data are from Ref. 9. (c) Comparison with the experimental data after the coupled-channel results have been folded with the experimental resolution; see Refs. 9 and 18.

for the transfer of the electron from the target ground state to the projectile continuum state as a function of the electron energy, where the impact parameter $b=0.36$ a.u. is chosen to correspond to the maximum contribution to $1s$-$1s$ charge transfer. The dots indicate the eigenenergies of the target continuum states in our pseudostate representation. It is impressive to see that the probability curve shows a sharp maximum at the energy E_m of momentum matching. The pseudostate corresponding to this energy will therefore be of primary importance for populating projectile states in a coupled-channel calculation. On the other hand, if we consider continuum excitation within the target, the resonant (momentum-matching) process occurring through the projectile ground state will be masked by nonresonant transitions.

Figure 3 shows differential $1s$-$1s$ capture cross sections obtained from coupled-channel calculations. In Fig. 3(a) we study the effect of excluding either the target continuum (dashed curve) or the projectile continuum (dash-dotted curve) from the coupled channels. In both cases we get almost identical cross-section curves showing a single Thomas peak at an angle slightly below the classical Thomas angle[1,3] of $\theta_{Th}=0.47$ mrad. This small shift may come about by the superposition upon a strongly sloping first-order curve. The solid curve, for comparison, represents the results of the complete coupled equations including both target and projectile Coulomb continua. In this case, we get an indication of a double-humped structure in the cross-section peak which presumably has to be attributed to the interference between both sequences in the two-path Thomas mechanism. It is interesting to note that the double-humped peak almost disappears (not shown here) if just the two matching states with energy E_m are discarded in the coupled equations while the whole rest of the continuum is kept. Of course, since our results have been obtained with a rather large but finite set of basis states, we cannot rule out the possibility that the dip in the twin structure may be washed out when the basis is further enlarged. This would not, however, affect our conclusion that target-centered and projectile-centered Coulomb continua contribute.

Figure 3(b) serves the purpose of comparing with the experimental data.[9] The solid curve [which is the same as in Fig. 3(a)] includes capture into $1s$, $2s$, $3s$, and $4s$ projectile states, while the experimental data contain transfer into *all* final states. The dash-dotted curve shows the result of an exactly evaluated second-order theory[7,8] (B2B0), while the dashed curve is obtained from exact second-order distorted-wave calculations (DWBA2), both satisfying Coulomb boundary conditions (see Ref. 8).

Figure 3(c) shows again the present theoretical results, however, now folded with the experimental resolution. The folding program[18] is the same one as used in the original experimental paper[9] in order to compare with other theories available at that time. We see that the agreement with the experimental results is remarkable, including forward angles which determine the total cross section. The theoretical values are 3.39×10^{-26} cm^2 for $1s$-$1s$ capture and 3.94×10^{-26} cm^2 for capture into $1s$, $2s$, $3s$, and $4s$ states. The experimental value[19] for capture into all final states is 3.1×10^{-26} cm^2.

In summary, we have demonstrated for the first time that the nonperturbative coupled-channel method can be

efficiently extended to very-high-lying continuum states by using a sufficiently large basis set of Gaussian-type orbitals. In this way, all interactions among the three charges are fully taken into account. The application of this method to the Thomas mechanism in $H^+ + H$ collisions at 5 MeV yields remarkable agreement with the experimental data. We have identified two distinct and interfering reaction paths, one through the target and one through the projectile Coulomb continuum, in each case with a resonance corresponding to momentum matching. As a next step, we plan to apply the method to higher angular momenta and to nonsymmetric collision systems.

The authors are indebted to F. Decker and W. Fritsch for helpful discussions. N.T. acknowledges a travel grant by the Hahn-Meitner Institute.

---

[a]Also at Fachbereich Physik, Freie Universität Berlin, D-1000 Berlin 33, Germany.

[1]L. H. Thomas, Proc. Roy. Soc. London A **114**, 561 (1927).

[2]R. M. Drisko, Ph.D. thesis, Carnegie Institute of Technology, 1955 (unpublished).

[3]R. Shakeshaft and L. Spruch, Rev. Mod. Phys. **51**, 369 (1979).

[4]P. R. Simony and J. H. McGuire, J. Phys. B **14**, L737 (1981); P. R. Simony, J. H. McGuire, and J. Eichler, Phys. Rev. A **26**, 1337 (1982); J. M. Wadehra, R. Shakeshaft, and J. Macek, J. Phys. B **14**, L767 (1981); J. E. Miraglia, R. D. Piacentini, R. D. Rivarola, and A. Salin, J. Phys. B **14**, L197 (1981).

[5]P. J. Kramer, Phys. Rev. A **6**, 2125 (1972); D. P. Dewangan, in *Electronic and Atomic Collisions,* edited by H. B. Gilbody *et al.* (North-Holland, Amsterdam, 1988); D. P. Dewangan and B. H. Bransden, J. Phys. B **21**, L353 (1988); F. Decker and J. Eichler, J. Phys. B **22**, L95 (1989).

[6]J. Macek and X. Y. Dong, Phys. Rev. A **38**, 3327 (1988); S. Alston, Phys. Rev. A **42**, 331 (1990).

[7]Dz. Belkic, Europhys. Lett. **7**, 323 (1988).

[8]F. Decker and J. Eichler, J. Phys. B **22**, 3023 (1989).

[9]H. Vogt, R. Schuch, E. Justiniano, M. Schulz, and W. Schwab, Phys. Rev. Lett. **57**, 2256 (1986).

[10]E. Horsdal-Pedersen, C. L. Cocke, and M. Stöckli, Phys. Rev. Lett. **50**, 1910 (1983).

[11]N. Toshima, Phys. Rev. A **42**, 5739 (1990).

[12]D. R. Bates and R. McCaroll, Proc. Roy. Soc. London A **245**, 175 (1958); W. Fritsch and C. D. Lin, in *Electronic and Atomic Collisions,* edited by J. Eichler, I. V. Hertel, and N. Stolterfoht (North-Holland, Amsterdam, 1984), p. 33; T. G. Winter and N. F. Lane, Phys. Rev. A **31**, 2698 (1985).

[13]See, e.g., M. R. C. McDowell and J. P. Coleman, *Introduction to the Theory of Ion-Atom Collisions* (North-Holland, Amsterdam, 1970).

[14]S. F. Boys, Proc. Roy. Soc. London A **200**, 542 (1950); H. Taketa, S. Huzinaga, and K. Oohata, J. Phys. Soc. Jpn. **21**, 2313 (1966); E. Clementi and G. Corongiu, Chem. Phys. Lett. **90**, 359 (1982).

[15]For an early reference in connection with a first-order Born approximation for charge exchange, see T. G. Winter and C. C. Lin, Phys. Rev. A **10**, 2141 (1974).

[16]L. F. Errea, L. Mendez, and A. Riera, J. Phys. B **12**, 69 (1979).

[17]K. Gramlich, N. Grün, and W. Scheid, J. Phys. B **22**, 2567 (1989).

[18]R. Schuch (private communication).

[19]W. Schwab, G. B. Baptista, E. Justiniano, R. Schuch, H. Vogt, and E. W. Weber, J. Phys. B **20**, 2825 (1987).